PHILOSOPHICAL TRANSACTIONS OF THE ROYAL SOCIETY A MATHEMATICAL, PHYSICAL & ENGINEERING SCIENCES

Fluid-dynamical and microscopic description of traffic flow: a data-driven comparison

Peter Wagner

Phil. Trans. R. Soc. A 2010 **368**, 4481-4495
doi: 10.1098/rsta.2010.0122

PHILOSOPHICAL TRANSACTIONS OF THE ROYAL SOCIETY A

Phil. Trans. R. Soc. A (2010) **368**, 4481–4495
doi:10.1098/rsta.2010.0122

Fluid-dynamical and microscopic description of traffic flow: a data-driven comparison

By Peter Wagner*

Institute of Transportation Systems, German Aerospace Centre, Rutherfordstraße 2, 12489 Berlin, Germany

Much work has been done to compare traffic-flow models with reality; so far, this has been done separately for microscopic, as well as for fluid-dynamical, models of traffic flow.

This paper compares directly the performance of both types of models to real data. The results indicate that microscopic models, on average, seem to have a tiny advantage over fluid-dynamical models; however, one may admit that for most applications, the differences between the two are small.

Furthermore, the relaxation times of the fluid-dynamical models turns out to be fairly small, of the order of 2 s, and are comparable with the results for the microscopic models. This indicates that the second-order terms are weak; however, the calibration results indicate that the speed equation is, in fact, important and improves the calibration results of the models.

Keywords: microscopic traffic-flow models; fluid-dynamical traffic-flow models; calibration

1. Introduction

Currently, there are about 100 traffic-flow models available; these fall into four classes: microscopic, mesoscopic, fluid-dynamical and truly macroscopic models. Several very good review articles exist, which describe them in more detail and their relationship with each other (Chowdhury *et al.* 2000; Helbing 2001; Nagel *et al.* 2003; Maerivoet & Moor 2005). On the most basic level, there are microscopic traffic-flow models, which model each individual vehicle–driver unit (or even more basic on the basis of a detailed vehicle dynamics). Mesoscopic models still usually have individual vehicles, but they drop the interaction between the vehicles in favour of an aggregated interaction between each vehicle and an averaged field. This average field can be the density profile $k(x,t)$, where k is the vehicle density that depends on the position x and the time t, or the speed profile $v(x,t)$ on a link. (In physicists parlance, this is a mean-field approach.) The fluid-dynamical models drop the individual vehicles in favour of fields and write down dynamical equations for the time evolution of the density $k(x,t)$ and the speed $v(x,t)$, while the macroscopic models, such as those used to do traffic planning, very often lack a concise dynamical description in terms of differential

*peter.wagner@dlr.de

One contribution of 10 to a Theme Issue ‘Traffic jams: dynamics and control’.

equations—users of these models are interested in average values only. Therefore, a whole road segment reduces to a so-called link performance function, relating demand and travel time or travel costs.

For each of the four classes defined above, a further subclassification is available. The microscopic models come as differential equations, time-discrete update equations, or even fully discrete cellular automata models, each with its own merits and short-comings. In the more physics-minded part of the traffic community, there is also the further subdivision into one-phase, two-phase or three-phase models. They differ in the details of the car-following dynamics: one-phase models always have a stable fixed point in car following, in two-phase models, there exist some values of the density where this fixed point becomes unstable, creating start-and-stop jam waves, while three-phase models (see Kerner 2004) have many marginally stable fixed points in car following, even for the same speed.

Fluid-dynamical models are classified into first-order models, which have only one partial differential equation for the density and an algebraic equation for the velocity, and second-order models, which have two partial differential equations for the density and velocity. Rarely, third-order models have been defined in the literature, where a third equation is constructed to describe the standard deviation of the speed.

In principle, this broad range of descriptions may lead to very different levels of realism for the different model classes. Therefore, this work tries to answer the question of what is lost when going from the microscopic to an aggregated level? To make this task manageable, the focus here is on a few representatives of the microscopic and the fluid-dynamical model classes.

2. Description of data and models

(*a*) *Data*

The data were chosen from the California freeway I-80 near Berkeley, CA, USA. The I-80 is a five-lane freeway, the data were chosen from a stretch without any on- and off-ramps. Figure 1 displays the geometry of the study area. To compare a model to reality, the following set-up is needed: two sets of data (from loop detectors here) provide the inflow and the outflow boundary conditions, while another detector in the middle of the study area measures the performance of the models by comparing the simulation results at this detector with the real data. The data from the detector located at the entry of the study area are used to drive the inflow end of the simulation, while the data from the last detector define the outflow condition. For a microscopic model, it is sufficient to use the speeds from the downstream end, and the flows from the upstream end. For fluid-dynamical models, both data (flows and speed) might be necessary; this depends on the model.

The data are from a five-lane road and had been aggregated into one single average speed and flow time series for the three detector locations in a time interval of 15 s, see Brockfeld *et al.* (2005). When comparing fluid-dynamical models with microscopic ones, this has the advantage that there is no need to use the generalization of the fluid-dynamical or the microscopic models to several lanes, which does not always exist. Of course, the microscopic models

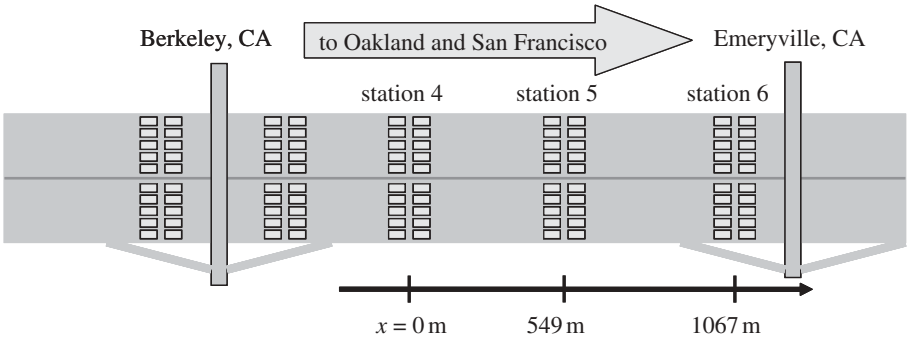

Figure 1. Sketch of the detector locations on the I-80 near San Francisco, CA, USA. Only the data of station numbers 4–6 have been used in the simulation study, with traffic flowing in the direction to San Francisco. The study area was 1067 m long, and station number 5 detectors are located at $x = 549$ m.

could be used to run a full multi-lane program; this work has also avoided this in order to compare just the longitudinal behaviour. An additional advantage gained by using aggregated data is that all models get the same input, and that it is easier for the microscopic models to insert vehicles into the simulation area with aggregated (smoothed) data. Very often, microscopic models do not allow for the small headways observed in real data and therefore generate a jam at the entrance of the simulation area since a following vehicle inserted with such a small headway forces an emergency brake.

In addition to this, the data selected present a strong challenge to the models since they display almost all types of different traffic-flow patterns, from free flow to highly congested flow. This can be seen, for example, in the space–time plot in figure 2, which has been generated with the help of the microscopic Stefan Krauss (SK) model after successful calibration of the data.

The approach that has been followed here does have limitations. In particular, more detailed questions regarding the microscopic interaction between vehicles cannot be answered in this manner, or more precisely, only to the effect they have on the macroscopic features. Owing to the nature of the chosen data, the following approach only compares the macroscopic features of the used microscopic models, i.e. their ability to reproduce the congestion patterns observed in the data.

Nevertheless, from a statistical point of view, the approach taken here seems valid: the dynamical complexity of a fluid-dynamical model (e.g. the numbers of equations needed) is comparable to the number of vehicles in the simulation area. In addition, the number of parameters is roughly the same, as long as it is assumed that the microscopic parameters are the same for each vehicle (for the microscopic case) or do not change with space and time (in the fluid-dynamical case).

(*b*) *Models*

Three microscopic and three fluid-dynamical models have been selected. It is hoped that they are sufficiently general to represent a large class of different traffic-flow models.

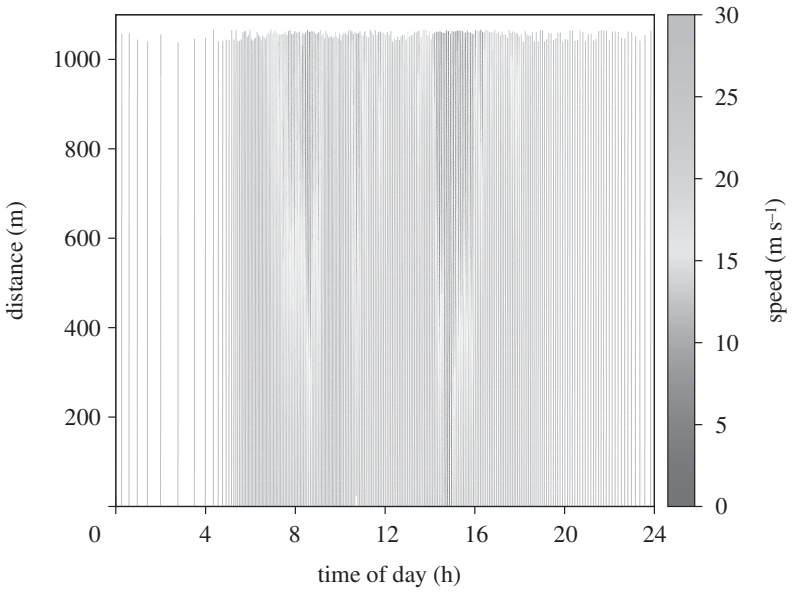

Figure 2. Space–time plot of the simulation with a microscopic model, after successful calibration. Shown is any 50th trajectory. It can be seen that there were two highly congested episodes over the day, where the traffic jam spanned the whole study area.

(i) *Microscopic traffic-flow models*

The microscopic models to be used in the following are of three different types: two fairly simple ones, and a much more complicated model as used in the Massachusetts Institute of Technology Simulator (MITSIM; Ahmed 1999; http://mit.edu/its/mitsimlab.html).

The first model to be used here is a generalization of the model introduced in Krauß *et al.* (1997). While the original version of this model can be used with a step size of 1 s only, the version below works for any time-step size Δt of the update scheme,

$$v_i(t+\Delta t) = \min\{v_{\max}, v_{\text{safe}}, a\Delta t + \sigma_{\text{a}}\sqrt{\Delta t}\xi_i(t)\}, \tag{2.1}$$

with

$$v_{\text{safe}} = -bh_{\text{pref}} + \sqrt{(bh_{\text{pref}})^2 + v_{i-1}^2 + 2bg_i}. \tag{2.2}$$

Here, v_i is the speed of vehicle i and $g_i = x_{i-1} - x_i - \ell_i$ is the distance between this vehicle and the lead vehicle $i-1$; ℓ_i is the generalized vehicle length, i.e. the physical length of the vehicle plus the distance between the vehicles in a traffic jam. The parameters used in this model are the maximum possible speed $v_{\max}$ of the vehicle, its maximum acceleration a and its maximum deceleration b, the preferred time headway h_{pref} and the acceleration noise σ_{a}. A random number $\xi_i(t)$ is drawn in any time step and for any vehicle, which makes the model a stochastic one. Note that sometimes the parameter h_{pref} has been interpreted as the reaction time; however, this is not the best possible interpretation: for a time-step size $\Delta t < h_{\text{pref}}$ that is needed for the crash-freeness

of the model, the time-step size Δt is the reaction time, while h_{pref} is in fact the equilibrium distance obtained when the driver does not need to accelerate ($v_i(t+\Delta t) = v_i(t)$).

This model is in fact a kinematic model, since the speed is assigned directly and there is no differential equation for the acceleration. Furthermore, it is the model that is used in the Simulation of Urban Mobility (SUMO) open-source simulator (http://sumo.sourceforge.net), and it shares some similarities with the model introduced in Gipps (1981).

The second model class has been first described in Bando *et al.* (1995). It states, that the reaction of the driver i depends only on the distance g_i (net headway) to the vehicle in front, and not (in addition) on the velocity difference between the vehicles,

$$\dot{v}_i = \frac{1}{T}(F(g_i) - v_i). \tag{2.3}$$

Here, the constant T is a relaxation time, which the current speed v_i needs to converge towards $F(g)$. The function $F(g)$ is sometimes named the optimal velocity (OV) function, and it typically has a sigmoid shape: it starts out slowly (for small distances g), then rises sharply (intermediate g), until it finally saturates at the maximum speed $v_{\max}$. Many different formulations are available for the OV function. Here, the one introduced in Orosz *et al.* (2004) will be used,

$$F(g) = v_{\max}\frac{(g/s)^3}{1+(g/s)^3}. \tag{2.4}$$

Here, the parameter s is a scaling parameter of the OV function.

From a microscopic point of view, models where drivers react to changes in distance only are definitely wrong, drivers react more strongly to the speed difference between the vehicles. Nevertheless, these types of models are very popular in the physical and mathematical literature because they are simple to analyse and understand, and even analytical results can be derived.

In the case of this model, there is also a related fluid-dynamical model at hand, which was first derived in Berg *et al.* (2000), therefore it will be named the Berg, Mason & Wilson (BMW) model in the following. This is another virtue of the OV models, it is fairly simple to connect such a microscopic model to its macroscopic counterpart—often, the correspondence between a microscopic and its fluid-dynamical counterpart is weaker than in this case.

These two microscopic models have a small number of parameters, the SK model has six and the BMW model has four parameters, see table 1 for details. This is no longer true for the third model, which is at the other end of the complexity scale.

This last model is used in the MITSIM simulator (http://mit.edu/its/mitsimlab.html); here, the version as described in Ahmed (1999) is used. It is a three-regime model, where the different driving regimes depend on distance: for small distances, drivers try to avoid crashing into the vehicle in front, for intermediate distances they follow the vehicle in front (according to a generalization of the General Motors (GM) model family defined in Gazis *et al.* (1961)), while for large distances, they drive uninfluenced with their own preferred maximum speed. The two thresholds that separate the three regimes are two time headways $h_{\mathrm{l}}, h_{\mathrm{u}}$, each drawn from a truncated normal distribution (called $\mathcal{N}(\mu, \sigma)$

Table 1. The parameters of the three models. Implicit means that there is no explicit parameter like $a_{\max}$ or $b_{\max}$, but it is built into the $F(g)$ function. Complex means that more than a single parameter is needed to describe this part of the model.

parameter	description	BMW	SK	MITSIM
$v_{\max}$	maximum speed	yes	yes	yes
$a_{\max}$	maximum acceleration	implicit	yes	yes
$b_{\max}$	maximum deceleration	implicit	yes	yes
ℓ	vehicle length	yes	yes	yes
σ_{a}	acceleration noise	no	yes	complex
h_{pref}	preferred headway	no	yes	yes
s	scaling parameter of the OV function	yes	no	no
T	relaxation time	yes	no	complex
T_{ff}	MITSIM free (relaxation time in free flow)	no	no	yes
$\alpha_{\pm}, \beta_{\pm}, \gamma_{\pm}, \rho_{\pm}$	MITSIM follow (exponents of the interaction term)	no	no	yes
$\lambda_{\pm}$	MITSIM follow (acceleration scaling factors)	no	no	yes
$\sigma_{\pm}$	MITSIM follow (acceleration noise)	no	no	yes
σ_{ff}	MITSIM free (acceleration noise in free flow)	no	no	yes

in the following) with a certain width $\sigma_{h_{\mathrm{l}}}$, $\sigma_{h_{\mathrm{u}}}$. So, the model reads (where $h = g/v$ is the current time headway)

$$a = \begin{cases} a_{\mathrm{brake}}, & \text{if } h < h_{\mathrm{l}}, \\ a_{\mathrm{follow}}, & \text{if } h_{\mathrm{l}} \le h < h_{\mathrm{u}}, \\ a_{\mathrm{free}}, & \text{if } h_{\mathrm{u}} \le h, \end{cases} \tag{2.5}$$

with the acceleration function defined as

$$a_{\mathrm{brake}} = \begin{cases} \min\left\{-b_{\max}, a_{i-1} - \dfrac{(\Delta v_i)^2}{2 g_i}\right\}, & \text{if } v_i > v_{i-1}, \\ \min\left\{-b_{\max}, a_{i-1} - \dfrac{b_{\max}}{4}\right\}, & \text{if } v_i \le v_{i-1}, \end{cases} \tag{2.6}$$

$$a_{\mathrm{follow}} = \lambda_{\pm} \frac{v_{i-1}^{\beta_{\pm}}(t-\tau)}{g_i^{\gamma_{\pm}}(t-\tau)} k^{\rho_{\pm}}(t-\tau) |\Delta v_i(t-\tau)|^{\alpha_{\pm}} + \mathcal{N}(0, \sigma_{\pm}) \tag{2.7}$$

and

$$a_{\mathrm{free}} = \frac{1}{T_{\mathrm{ff}}}(v_{\max} - v(t-\tau)) + \mathcal{N}(0, \sigma_{\mathrm{ff}}). \tag{2.8}$$

In equation (2.7), the sign $\pm$ stands for the different signs of the speed difference $\Delta v_i = v_{i-1} - v_i$. The variable k is an approximation to the density in front of the vehicle, the variable τ is the reaction time, which has been set to zero in the

calibration below. Note in addition, that this model assumes that the driver can estimate the acceleration of the lead driver, which in general seems difficult for human drivers to do.

(ii) *Fluid-dynamical traffic-flow models*

The arguably most simple of all fluid-dynamical descriptions is the kinematic-wave model (Lighthill & Whitham 1955; Richards 1956). It is the consequence of vehicle conservation, which was stated first by Lighthill & Whitham (1955),

$$\partial_t k(x,t) = -\partial_x q(x,t). \tag{2.9}$$

In this equation (2.9), $k(x,t)$ denotes the density of vehicles as a function of space x and time t, while the $q(x,t)$ is the traffic flow, i.e. the numbers of vehicles that pass a given cross section of the road under consideration. Within this theory, it is assumed that the speed field $v(x,t)$ of the traffic stream adopts immediately to the density k. Since traffic flow, density and speed are related by the relation $q = kv$, this means that the traffic flow is a function of density $q(k)$, which is called the fundamental diagram of traffic flow. In the original paper, see Lighthill & Whitham (1955), the fundamental diagram is a simple triangular function: for traffic density below a critical density, the observed flow increases with density linearly, with the slope equal to the maximum speed of the traffic stream, while above the critical density, the traffic flow declines with density until it finally reaches zero. This time, the slope of the decline is the speed of the backward-travelling jam wave. Note, however, that more general fundamental diagrams may exist, or even none at all (Kerner 2004).

The model in equation (2.9) is already an acceptable description of traffic flow from a macroscopic point of view. However, in cases where traffic flow is highly dynamic, e.g. in the case of stop-and-go waves, this description had to be enhanced by an additional differential equation that describes the dynamics of the velocity field $v(x,t)$. This then defines the second-order fluid-dynamical equations of traffic flow; the earliest one was given in Payne (1971),

$$\partial_t k(x,t) = -\partial_x q(x,t) \tag{2.10}$$

and

$$\partial_t v(x,t) = \frac{1}{T}(V(k(x,t)) - v(x,t)) - \frac{c^2}{k(x,t)}\partial_x k(x,t), \tag{2.11}$$

where $V(k)$ is an assumed equilibrium speed–density relationship and $(c^2/k)\partial_x k$ is a term that describes anticipation of the driver to the density downstream of the current location x. The function $V(k)$ has an intimate relationship with the OV function introduced above in the case of the BMW model, in fact for homogeneous traffic (no acceleration), the two coincide and are equal to the fundamental diagram introduced above. The density is the inverse of the average distance plus the average vehicle length, $k = 1/(\langle g\rangle + \langle \ell\rangle)$.

The approach of Payne (1971) will not be used here, instead more modern approaches will be considered. Note that there is an ongoing discussion (see Zhang 2009 for an overview) centred around the drawbacks of most of the second-order models (which was initiated by Daganzo 1995).

In numerical analyses, these partial differential equations need to be discretized, and these discretizations are used in the rest of this work.

To start, first the kinematic-wave model will be used in the approximation derived in Daganzo (1994), the cell transmission (CT) model. As for all fluid-dynamical models, the street is divided into cells of a certain length L; usually, L may be selected in the range between 50 and 500 m. At each time t, and within each cell ν, there is a certain number $n_\nu(t)$ of vehicles present, which can be non-integer values. Each cell also has a maximum capacity N_ν, i.e. it cannot hold more vehicles than that. The number of vehicles that can be transferred between a cell ν and its downstream cell $\nu+1$ in a time step Δt is then determined by the following relationship:

$$q_{\nu\to\nu+1} = \min\{S(n_\nu), R(n_{\nu+1})\}, \tag{2.12}$$

where $S(\cdot)$ and $R(\cdot)$ are the sending and receiving functions, which describe what the upstream cell can send, and what the downstream cell is able to receive. These two functions become fairly simple if the cell length is chosen to be $L = v_{\max}\Delta t$, where $v_{\max}$ is the maximum speed of the stream, and if the underlying fundamental diagram of the modelled system is triangular,

$$S(n_\nu) = n_\nu \tag{2.13}$$

and

$$R(n_{\nu+1}) = w(N_{\nu+1} - n_{\nu+1}). \tag{2.14}$$

In this equation, w is the speed of the backward-running jam wave, normalized to the maximum speed, $w = \tilde{w}/v_{\max}$.

As discussed above, the CT model as a first-order fluid-dynamical model assumes that the speed adapts instantaneously to a change in density, a fact that is apparently not true. Therefore, generalizations to this model also include a dynamical equation for the speed. Here, two approaches will be used that are not affected by the criticism in Daganzo (1995). The first one is a model described in Hilliges & Weidlich (1995) (called HILL in the following), and a model described in Aw & Rascle (2000) (called AR in the following), developed as an explicit mathematical approach to respond to Daganzo (1995) and to counteract the drawbacks of the second-order fluid-dynamical approaches. The HILL model is defined similar to the CT model,

$$L\dot{k}_\nu = k_{\nu-1}v_\nu - k_\nu v_{\nu+1} \tag{2.15}$$

and

$$\dot{v}_\nu = \frac{1}{T}(V(k_\nu) - v_\nu) + \frac{v_\nu}{2L}(v_{\nu-1} - v_{\nu+1}), \tag{2.16}$$

but with an explicit second-order term for the speed relaxation, which is again the term similar to the OV function of the BMW model. The variable k_ν is different from the CT model, it is now the traffic density in each of the cells.

The final model to be considered here is the AR model, see Aw & Rascle (2000). It is defined by

$$\partial_t k(x,t) = -\partial_x q(x,t) \tag{2.17}$$

and

$$\partial_t v(x,t) = -v(x,t)\partial_x v(x,t) + k(x,t)p'(k(x,t))\partial_x v(x,t). \tag{2.18}$$

These three models (CTM, HILL, AR), together with their explicit discretization as described in the respective articles (Daganzo 1994; Hilliges & Weidlich 1995; Aw & Rascle 2000), are used as representatives of the fluid-dynamical class of models.

(*c*) *Boundary conditions*

As mentioned already, the boundary conditions need to be given by the external data, therefore the model under consideration is driven by the external data. The data from loop detectors provide traffic flow $q_{\mathrm{in}}(t)$, $q_{\mathrm{out}}(t)$ and speed $v_{\mathrm{in}}(t)$, $v_{\mathrm{out}}(t)$ as primary measured variables, from which the third variable for the description of traffic flow, the density, can be derived. (Strictly speaking, computing the density by $k = q/v$ is only allowed if the traffic stream is homogeneous.) A microscopic model definitely needs the inflow $q_{\mathrm{in}}(t)$, the speed is not really needed since it is a consequence of the vehicle dynamic downstream of the insertion point and the insertion mechanism itself. The insertion is done as follows (see Namazi *et al.* (2002) and references therein for a discussion of insertion rules): at any time step, when a vehicle must be inserted (according to the data), the last vehicle in the system must be considered; if it is far enough within the system so that the newly inserted vehicle is not influenced by its downstream predecessor, the new vehicle can be set at the beginning of the study area. This is done with the maximum speed possible, and the vehicle will adapt, after a few seconds, to the speeds within the study area. If the last vehicle is too close, the newly inserted vehicle will be set a certain distance upstream of the study area, which, for this purpose, must be part of the simulation area—the condition is that the distance had to be chosen such that the new vehicle can be inserted with a speed larger or equal to the speed of its predecessor. If there is a mismatch between the simulation and the data, vehicles at the entrance may 'pile up', leading finally to a bad measure of performance for this simulation run and this model; this may be corrected by adopting the parameters of the model until a good fit is reached and little or no vehicles jam at the entrance.

The downstream condition is simpler to realize: it has to be ensured that the vehicles leave the simulation area with a speed as large as the measured one $v_{\mathrm{out}}(t)$. This is simple to accomplish, and it is important: if the study area is homogeneous and if there is no bottleneck in it (as is the case for the I-80 study area used in this work), it is impossible with most microsimulation models to generate a traffic jam within the study area. Therefore, the jams observed in the data are imported, i.e. they are generated downstream (in this case, by the toll station of the San Francisco Bay Area bridge) and travel backwards into the study area—the reduced speeds at the onset of such a jam are exactly the mechanism that transport them into the study area.

In principle, also the traffic flow $q_{\mathrm{out}}(t)$ at the outflow could have been used as a boundary condition. This is not as straightforward as using the speeds since it has to be ensured that no more than the measured flow $q_{\mathrm{sim,out}}(t) \leq q_{\mathrm{out}}(t)$ leaves the study area. This can again be reached by an appropriately set speed limit, or by changing the preferred headway of the leading vehicle that slows it down, or, finally, by using a virtual traffic light (Brockfeld *et al.* 2003) that enforces the condition $q_{\mathrm{sim,out}}(t) \leq q_{\mathrm{out}}(t)$. However, this causes a strong disturbance in the traffic flow and should be done only if nothing else works, e.g. if speed data are not available.

(*d*) *Calibration/validation: optimization issues*

Any model contains a set of parameters $\mathbf{p} := \{p_i\}$ that can be used to adopt to the scenario at hand. In general, running each of the models with its set of parameters, and with the boundary conditions set by the empirical data, it produces a speed measurement $v_k^{\mathrm{sim}}(\mathbf{p})$ at the loop detectors of station number 5, which can be compared with the real data v_k^{emp},

$$e(\mathbf{p}) = \sum_{i=k}^{M} \left(\frac{v_k^{\mathrm{sim}}(\mathbf{p}) - v_k^{\mathrm{emp}}}{v_k^{\mathrm{emp}}} \right)^2, \tag{2.19}$$

which defines the root mean square (r.m.s.) error with M being the number of data points. Other measures of performance (Brockfeld *et al.* 2003, 2005; Toledo *et al.* 2007) might be used and may influence the outcome of the calibration task, see Brockfeld *et al.* (2004), Toledo *et al.* (2004), Hoogendoorn & Ossen (2005) and Ossen & Hoogendoorn (2007). Note that for the models considered here, a homogeneity assumption has been made: all vehicles for the microscopic models share the same set of parameters, and the same is true for the fluid-dynamical models: all parameters are kept constant over the simulation time (one day) and the simulation area.

To find the optimum set of parameters for each model, the equation (2.19) has to be minimized with respect to this set of parameters $\mathbf{p}$. For this nonlinear optimization, several tools are available (e.g. Press *et al.* 2007). The results of this minimization, of course, are now the optimized parameters for the scenario at hand. So, in a final step, it is usually necessary to apply a model with a fitted set of parameters to a different scenario and see how well it fits there—without adapting the parameters once more. This final step is called validation, and usually the validation results are another 5 per cent worse than the calibration results (Brockfeld *et al.* 2003, 2004, 2005). Within this work, only calibration results will be provided, since a direct comparison between fluid-dynamical and microscopic models is undertaken. A typical result is shown in figure 3; here, the time series of the data at station number 5 is compared with the simulation results after successful minimization.

As can be seen in figure 3, but much more clearly in the space–time plot in figure 2, the situation at this test site is highly congested, causing a strong challenge for all the models. All the simulations were run over the whole day, in order to collate different situations that have to be described by the models. Furthermore, four additional days of data have been analysed, which yield quite comparable results.

3. Results

The results are displayed in figure 4. It can be seen that the best model is a simple microscopic model; its r.m.s. error is around 11 per cent, which is a fairly good value in comparison with the results obtained for more microscopic car-following data (Brockfeld *et al.* 2003, 2004). From Brockfeld *et al.* (2005), it is known that other simple microscopic models can also reach this r.m.s. error. In general, there is a tendency that models with fewer parameters perform better

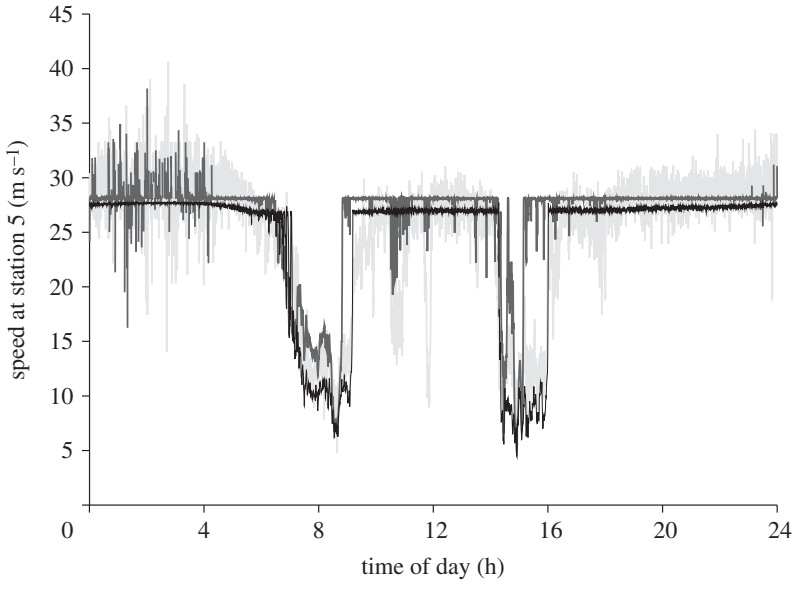

Figure 3. Time series of the data (light grey), and two of the six models (SK: grey, HILL: black) investigated here.

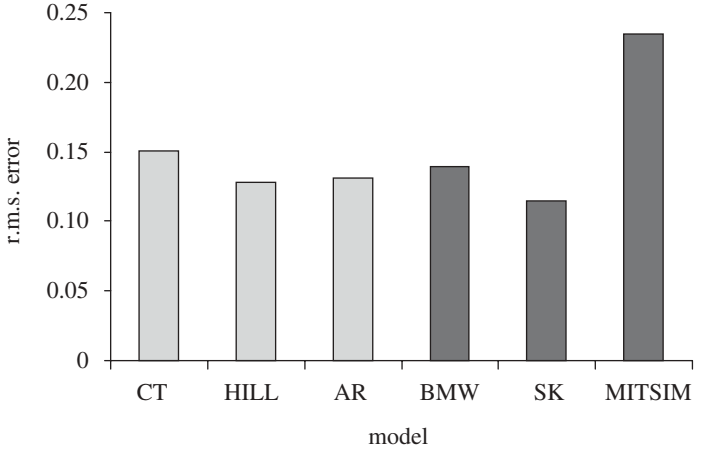

Figure 4. The r.m.s. error of the six models, with the fluid-dynamical ones in black and the microscopic ones in grey. Note that the results have not been corrected for the number of parameters by using, for example, Akaike's information criteria (Akaike 1974) as an additional calibration objective.

than models with more parameters; this might be an effect of the limitations in the optimization routines—they do not deal very well with the high-dimensional optimization, since it is very probable that a large parameter space is riddled with local minima (see especially the results obtained for the MITSIM model). The

CT model is the weakest among the fluid-dynamical models and it seems that a simple second-order term improves the fluid-dynamical model. Nevertheless, the improvement is not very large, even the CT model seems to gather most of the patterns displayed by the traffic flow in this study area.

One of the surprising results is the magnitude of the relaxation parameter T of the fluid-dynamical models. On average, it is somewhere between 1 and 3 s. It turns out that this result seems to be generally correct, as a more detailed analysis for the HILL model and the analysis below demonstrates. The relaxation time for this model where the objective function $e(\mathbf{p})$ is minimal is around $T = 2.8$ s. This is in line with the numbers obtained for the microscopic models, which are typically around 1–2 s, as well as for the relaxation times and for the preferred headways. For a discussion on the interplay between reaction times, relaxation times and preferred headways, see Kesting & Treiber (2008).

Finally, note that reaction times are much more difficult to assess. In normal driving circumstances, drivers anticipate quite correctly what will happen during the next couple of seconds, and therefore do not need to react in the classical sense of being surprised and need some time to cope with a new un-anticipated event. There are even examples, e.g. when drivers approach a red traffic light, where reaction times are negative since the following driver starts braking before the lead driver.

(*a*) *Relaxation times*

So far, the analysis of relaxation times has been completely based on the calibration results. Here, another data source of single vehicle data will be used to support the results of the calibration by an empirical analysis. By looking at single-vehicle data, the question of how fast does the speed change from one vehicle to the next one in a traffic stream may be asked. This is relevant for the models above, since they have been driven by exactly this kind of data—only changes in speed that are within the data trigger changes in the models, and do therefore influence the relaxation time of the models.

To answer this question, for each pair of vehicles following each other, a kind of acceleration (called the acceleration index in the following) may be computed. Let v_i be the speed of the ith vehicle in a traffic stream and v_{i+1} be the speed of the following vehicle, which follows with a time headway of h_i. Then, the acceleration index (the letter $\alpha_i = (v_{i+1}(t + \tau_i) - v_i(t))/\tau_i$ is used here to differentiate it from normal accelerations) can be defined and analysed. It turns out that α is relatively constant: in most cases, the acceleration index values are bounded to $-1 \leq \alpha \leq 1\,\mathrm{m\,s^{-2}}$, and acceleration values larger than $|\alpha| > 2$ could not be observed in this dataset.

This analysis is summarized in figure 5, where the averaged acceleration index between subsequent vehicles passing a double-loop detector is plotted. Therefore, typical acceleration values are quite small, and from the simple differential equation $\dot{v} = (V(\cdot) - v)/T$, it follows that T should be a function of the difference between the actual speed of the vehicle and the equilibrium speed $V(\cdot)$. For the data that has been analysed here, mostly small speed differences between subsequent vehicles $|\Delta v| \leq 5\,\mathrm{m\,s^{-1}}$ are observed. The acceleration index $\alpha \leq 2\,\mathrm{m\,s^{-2}}$ is also bounded, so that the empirical relaxation time $T \approx \Delta v/\alpha$ is of the order of 2–3 s, in line with the calibration results above.

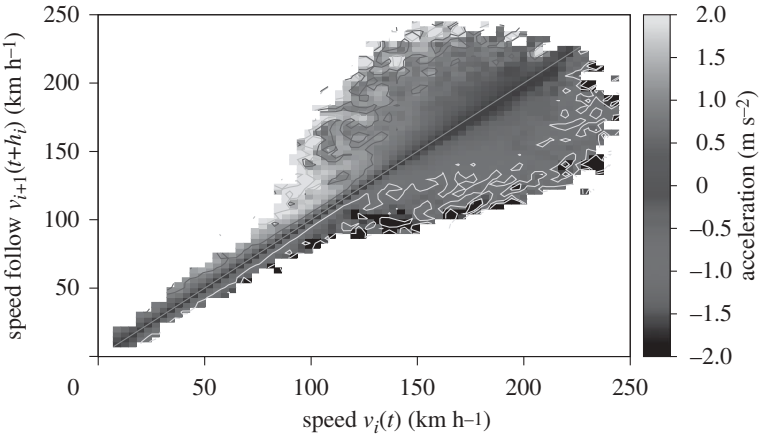

Figure 5. Contour plot of the acceleration values as a function of $v_i(t)$ and $v_{i+1}(t + h_i)$. Almost all pairs $v_i(t), v_{i+1}(t + h_i)$ are distributed along the diagonal, except for larger speeds where the distances between the vehicles grow, and therefore larger speed differences can occur.

4. Conclusions and outlook

It has been shown in this work that fluid-dynamical and microscopic models yield quite comparable calibration results, where the simpler microsimulation models display a small advantage over the best fluid-dynamical models within this study. Therefore, it could be expected that microsimulation models which model the traffic flow as multi-lane flow might yield further improvements, since they can deal easier with inhomogeneities in the driver population. In most practical applications, the accuracy achieved here might be sufficient so that the analyst can chose any model, with a certain preference for the simpler ones.

There are several directions for generalization of these results. First of all, different places should be looked at, especially interesting are longer stretches of road where more details on the evolution of traffic-flow patterns can be observed, which will create stronger challenges for the models than the very short stretch used here. The modelling of the parameters as distributions is another important issue that brings with it the question of which is the correct measure of performance in such a situation? Even the current models, especially the ones with a stochastic update rule already create a difficult task for the optimization routines, which deal better with noise-less objective functions.

Furthermore, in addition to one-lane microscopic models, multi-lane-based models should be tested to see whether they could improve the results obtained so far. In any case, it is important to always use the comparative approach of comparing different models with the same type of data since it might be very hard to use absolute values.

Interestingly, the general results (11–15% r.m.s. error) are well within the bounds given by earlier results. It is not clear right now whether this is a kind of limit to how well a traffic-flow model can approximate real traffic data. In the long run, it is highly interesting to find out the limits in accuracy of traffic-flow modelling.

References

Ahmed, K. I. 1999 Modelling drivers' acceleration and lane-changing behaviour. PhD thesis, Department of Civil and Environmental Engineering, Massachusetts Institute of Technology, USA.

Akaike, H. 1974 A new look at the statistical model identification. *IEEE Trans. Autom. Control* **19**, 716–723. (doi:10.1109/TAC.1974.1100705)

Aw, A. & Rascle, M. 2000 Resurrection of second order models of traffic flow. *SIAM J. Appl. Math.* **60**, 916–938. (doi:10.1137/S0036139997332099)

Bando, M., Hasebe, K., Nakayama, A., Shibata, A. & Sugiyama, Y. 1995 Dynamical model of traffic congestion and numerical simulation. *Phys. Rev. E* **51**, 1035–1042. (doi:10.1103/PhysRevE.51.1035)

Berg. P., Mason, A. & Woods, A. 2000 Continuum approach to car-following models. *Phys. Rev. E* **61**, 1056–1066. (doi:10.1103/PhysRevE.61.1056)

Brockfeld, E., Kühne, R., Skabardonis, A. & Wagner, P. 2003 Towards a benchmarking of microscopic traffic flow models. *Transp. Res. Rec.* **1852**, 124–129. (doi:10.3141/1852-16)

Brockfeld, E., Kühne, R. & Wagner, P. 2004 Calibration and validation of microscopic traffic flow models. *Transp. Res. Rec.* **1876**, 62–70. (doi:10.3141/1876-07)

Brockfeld, E., Kühne, R. & Wagner, P. 2005 Calibration and validation of microscopic traffic flow models. *Transp. Res. Rec.* **1934**, 179–184. (doi:10.3141/1934-19)

Chowdhury, D., Santen, L. & Schadschneider, A. 2000 Statistical physics of vehicular traffic and some related systems. *Phys. Rep.* **329**, 199–329. (doi:10.1016/S0370-1573(99)00117-9)

Daganzo, C. F. 1994 The cell transmission model: a simple dynamical representation of highway traffic. *Transp. Res. B* **28**, 269–287. (doi:10.1016/0191-2615(94)90002-7)

Daganzo, C. F. 1995 Requiem for second-order fluid approximations of traffic flow. *Transp. Res. B* **29**, 277–286. (doi:10.1016/0191-2615(95)00007-Z)

Gazis, D. C., Herman, R. & Rothery, R. W. 1961 Nonlinear follow-the-leader models of traffic flow. *Oper. Res.* **9**, 545–567. (doi:10.1287/opre.9.4.545)

Gipps, P. G. 1981 A behavioural car following model for computer simulation. *Transp. Res. B* **15**, 105–111. (doi:10.1016/0191-2615(81)90037-0)

Helbing, D. 2001 Traffic and related self-driven many-particle systems. *Rev. Mod. Phys.* **73**, 1067–1141. (doi:10.1103/RevModPhys.73.1067)

Hilliges, M. & Weidlich, W. 1995 A phenomenological model for dynamic traffic flow in networks, *Transp. Res. B* **29**, 407–431. (doi:10.1016/0191-2615(95)00018-9)

Hoogendoorn, S. P. & Ossen, S. 2005 Parameter estimation and analysis of car-following models. In *Transportation and traffic theory: flow, dynamics and human interaction*, *Proc. 16th Int. Symp. on Transportation and Traffic Theory* (ed. H. S. Mahmassani), pp. 245–265. Amsterdam, The Netherlands: Elsevier.

Kerner, B. S. 2004 *The physics of traffic*. Berlin, Germany: Springer.

Kesting, A. & Treiber, M. 2008 How reaction time, update time and adaptation time influence the stability of traffic flow. *Comp. Aided Civ. Infrastruct. Eng.* **23**, 125–137.

Krauß, S., Wagner, P. & Gawron, C. 1997 Metastable states in a microscopic modelling of traffic flow. *Phys. Rev. E* **55**, 5597–5606. (doi:10.1103/PhysRevE.55.5597)

Lighthill, M. J. & Whitham, J. B. 1955 On kinematic waves. II: a theory of traffic flow on long crowded roads. *Proc. R. Soc. Lond. A* **229**, 317–345. (doi:10.1098/rspa.1955.0089)

Maerivoet, S. & De Moor, B. 2005 Transportation planning and traffic flow models. (http://www.arxiv.org/abs/physics/0507127).

Nagel, K. Wagner, P. & Woesler, R. 2003 Still flowing: approaches to traffic flow and traffic jam modeling, *Oper. Res.* **51**, 681–710. (doi:10.1287/opre.51.5.681.16755)

Namazi, A., Eissfeldt, N., Wagner, P. & Schadschneider, A. 2002 Boundary-induced phase transitions in a space-continuous traffic model with non-unique flow-density relation. *Eur. Phys. J. B* **30**, 559–570. (doi:10.1140/epjb/e2002-00414-4)

Orosz, G., Wilson, R. E. & Krauskopf, B. 2004 Global bifurcation investigation of an optimal velocity traffic model with driver reaction time. *Phys. Rev. E* **70**, 026207. (doi:10.1103/PhysRevE.70.026207)

Ossen, S. & Hoogendoorn, S. P. 2007 Calibrating car-following models using microscopic trajectory data: a critical analysis of both microscopic trajectory data collection methods and calibration studies based on these data. Report T & P 2006.010. Delft University of Technology, Delft, The Netherlands.

Payne, H. J. 1971 Models of freeway traffic and control. *Math. Models Public Syst.* **28**, 51–61.

Press, W. H., Teukolsky, S. A., Vetterling, W. T. & Flannery, B. P. 2007 *Numerical recipes—the art of scientific computing*, 3rd edn. Cambridge,UK: Cambridge University Press.

Richards, P. I. 1956 Shockwaves on the highway. *Oper. Res.* **4**, 42–51. (doi:10.1287/opre.4.1.42)

Toledo, T., Ben-Akiva, M., Darda, D., Jha, M. & Koutsopoulos, H. N. 2004 Calibration of microscopic traffic simulation models with aggregate data. *Transp. Res. Rec.* **1876**, 10–19. (doi:10.3141/1876-02)

Toledo, T., Koutsopoulos, H. N. & Ben-Akiva, M. 2007 Integrated driving behaviour modeling. *Transp. Res., Part C: Emerg. Technol.* **15**, 96–112. (doi:10.1016/j.trc.2007.02.002)

Zhang, H. M. 2009 Comment on 'On the controversy around Daganzo's requiem for and Aw–Rascle's resurrection of second-order traffic flow models' by D. Helbing & A. F. Johansson, What faster-than-traffic characteristic speeds mean for vehicular traffic flow. *Eur. Phys. J. B* **69**, 563–568. (doi:10.1140/epjb/e2009-00183-6)